

# Numerical Simulation of Thermoelectric Refrigeration Materials

R. Sabarish\*

Department of Mechanical Engineering, Bharath University, Chennai-600 073, Tamil Nadu, India;  
sabarish.mech@bharathuniv.ac.in

## Abstract

This paper focuses on designing thermoelectric cooler via numerical method. Thermoelectric module in this study was made from (1) both side Sb<sub>2</sub>Te<sub>3</sub>. (2) Both side Bi<sub>2</sub>Te<sub>3</sub>. (3) p-side Sb<sub>2</sub>Te<sub>3</sub> and n-side Bi<sub>2</sub>Te<sub>3</sub>. The couple field equations were formulated in to system of algebraic by means of finite element method. Bi-Te and Sb-Te thermoelectric modules were considered for analyzing their performance. The current and temperature differences between the hot side and cold side were varied to study the characteristics of the thermoelectric module to analyze the maximum heat absorbed and maximum COP within the differential temperature. The numerical simulation is carried out by using finite element package ANSYS V13.

**Keywords:** Figure of Merit, Material Properties, Numerical Simulation, Peltier Cooling, Temperature, Voltage

## Nomenclature

$C$	heat capacity (J/Kg K)
$E$	electrical field (V/m)
$I$	current (A)
$J$	current density (A/m <sup>2</sup> )
$K$	thermal conductivity (W/cm K)
$N$	element shape function
$Q$	heat flux (W/m <sup>2</sup> )
$Q$	internal heat generation (W)
$T$	times (S)
$T$	temperature (K)
$Z$	figure of merit
QC	heat absorbed at cold side (W)
COP	coefficient of performance

## Greek symbols

$\Sigma$	electrical resistivity(S/m)
$A$	see beck coefficient (V/K)
$E$	electric permittivity (F/m)
$P$	density (Kg/Cm <sup>3</sup> )
$\Pi$	Peltier coefficient (J/V)

\* Author for correspondence

## 1. Introduction

Thermoelectric systems have been the subject of major advances in recent years, mainly due to develop the semiconductor material and the incorporation thermoelectric devices into domestic appliances. The thermoelectric coolers are solid state heat pumps, which remove heat from one side to dissipate the heat another side. This process is general, governed by reversible and irreversible thermal to electrical energy transformations. The main reversible effect is the peltier effect. The peltier effect determines the cooling potential of the device, whereas the reversible Joule heating and Fourier effect degrade the overall cooling performance<sup>1</sup>.

No moving parts of the thermoelectric system. Its maximum life approximately is 10<sup>5</sup> hrs of operation at 100°C and longer life at the lowest temperatures<sup>2</sup>. Some of the advantages of thermoelectric refrigeration system are precise temperature control, the ability to lower to the temperature below the ambient, controlled heat transport by current input and ability to be operative at any orientation. Their compact size makes them useful for applications where size or weight is a constraint,

the ability to alternate between heating and cooling is important and an excellent cooling alternative to vapor compression cooler is needed for systems that are sensitive to mechanical vibration. The electronic, medical, aerospace and telecommunications industries are other important areas for thermoelectric cooling applications<sup>3,4</sup>.

The thermoelectric cooler are based on the peltier effect; when a voltage or DC current is applied to dissimilar materials, a circuit can be created that allows continuous heat transport between the conductors junctions. The see beck effect is the peltier effect<sup>5</sup>.

The current is transport through the charge carriers (in the direction opposite to the hole flow or in that of electron flow). Heat transfer through the depending upon direction of the current. The efficiency of a thermoelectric material<sup>6</sup> is given by the figure of merit,

$$Z = \frac{\alpha^2 \sigma}{K} \tag{1}$$

The see beck coefficient ( $\alpha$ ), is given by Equation 2.

$$\alpha = \frac{E}{dT/dX} \tag{2}$$

Thermoelectric cooler material low electrical resistivity and thermal conductivity are required for a high figure of merit. These values are temperature dependent. Therefore, the figure of merit depends on the temperature. P and N type thermoelectric materials have different figures of merit and are averaged to determine

the materials overall quality<sup>6</sup>.

The present work a one dimensional steady state thermoelectric cooling problem, with a single par thermoelectric module was considered or the analyses as shown in Figure 1. The thermoelectric material properties vary with absolute temperature. Heat is absorbed in the cooling surface maintained at temperature  $T_c$  and heat is rejected by heated surface, maintained at temperature  $T_h$ . Bismuth Tellurium (Bi-Te) and Antimony Tellurium (Sb-Te) with across sectional area  $0.5 \times 0.5 \text{mm}^2$  and length of  $0.105 \text{mm}$  were considered as solid thermoelectric P and N semiconductor materials. In this project main objectives analysis of (1) to determine the maximum cooling power, maximum COP and maximum performance of parameters, (2) develop a computational model that simulates the thermoelectric refrigeration materials, (3) varying the operating parameters current and differential temperature and (4) compare the performance of the Bi-Te and Sb-Te thermoelectric module.

## 2. Computational Details

The equations to be describing the behavior of a thermoelectric material are governed by the couple equations of heat transfer and the continuity of current density phenomena, which are given by Equation 4. And

$$\rho c \frac{\partial T}{\partial t} + \nabla \cdot \vec{q} = Q \tag{3}$$

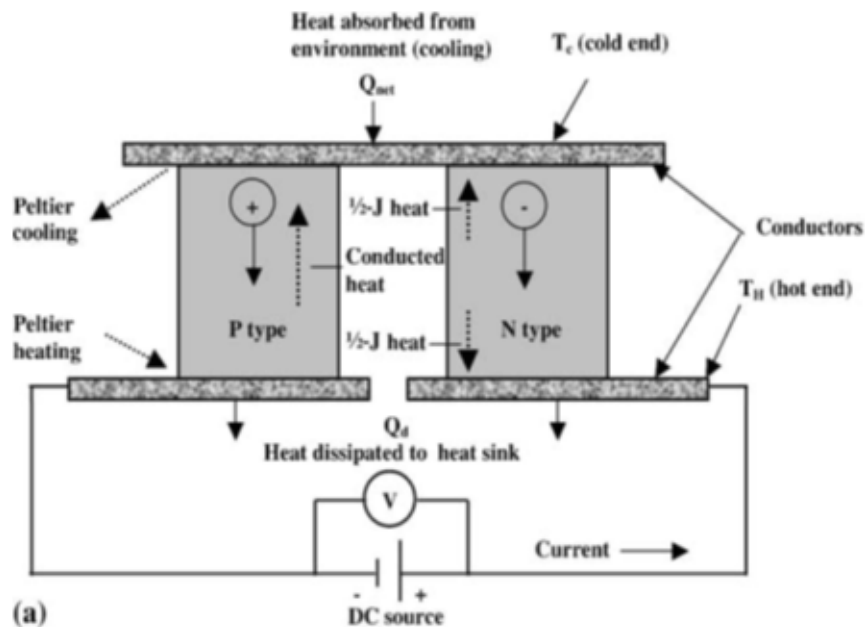


Figure 1. Single couple thermoelectric module.

$$\nabla \cdot (\epsilon \frac{\partial E}{\partial t}) + \nabla \cdot \bar{J} = Q \tag{4}$$

The electrical current density is generated by the coupling of the irreversible Joule effect and the reversible seebeck effect, as shown in Equation 5.

$$\bar{J} = \sigma \bar{E} - \sigma \alpha \nabla T \tag{5}$$

The heat flux  $q$  is generated by the reversible Peltier and irreversible Fourier effect, as shown in Equation 6.

$$\bar{q} = \pi \bar{J} - K \nabla T \tag{6}$$

The electrical field  $E$  is derived from the electric scalar potential  $\bar{\phi}$  as shown in Equation 7.

$$\bar{E} = -\nabla \phi \tag{7}$$

Finite element equations are transformed from the two coupled governing Equations 3 and 4 by approximating the primitive unknowns, temperature  $T$  and electrical  $\phi$ , into interpolation functions, and the value of the nodal known on an element as shown in Equations 8 and 9.

$$T = [N] \{T_e\} \tag{8}$$

$$\phi = [N] \{\phi_e\} \tag{9}$$

Where  $\phi_e$  the vector of nodal electrical potential is,  $T_e$  is the vector of nodal temperature, and  $N$  is the element shape function. After the manipulations based on the galerkin weighting scheme<sup>5</sup>, the differential equations (from Equations 7 to 9) become algebraic finite element equations as shown in Equation 10.

$$\begin{bmatrix} C_T & 0 \\ 0 & C_E \end{bmatrix} \begin{bmatrix} \frac{\partial T^2}{\partial t} \\ \frac{\partial \phi^2}{\partial t} \end{bmatrix} + \begin{bmatrix} K_T & 0 \\ K_{ET} & K_E \end{bmatrix} \begin{bmatrix} T_e \\ \phi_e \end{bmatrix} = \begin{bmatrix} Q \\ 1 \end{bmatrix} \tag{10}$$

The global matrix equation is ordered from the

individual finite element equations. The solution yields temperature,  $T_e$  and,  $\phi_e$  at unconstrained nodes or reactions in the form of the electric current and at nodes with the imposed electric potential and temperature respectively<sup>1</sup>.

The thermoelectric module is made of (1. both side  $Bi_2Te_3$ , and 2.  $Sb_2Te_3$  Then 3. n-side  $Sb_2Te_3$  and p-side  $Bi_2Te_3$ ) for n- and p-type leg, respectively. The module is created by connect n-and p-cells with thin copper plates on the top and bottom sides of its structure to establish the electrical contact between the cells, copper plate are served as substrate and supporting floor<sup>2</sup>. The n-and p-leg was similar dimension of  $4 \times 4 \times 0.15 \text{mm}^3$ . The height of n-and p-leg are 4mm. The copper plate size.

**Table 1.** Material properties

Material properties	$Bi_2Te_3$	$Sb_2Te_3$	Al	Sic
Density (kg/ m <sup>3</sup> )	7700	6500	2700	3210
Sp. Heat Capacity (J/kg-K)	155	210	900	750
Thermal Conductivity (W/m-K)	1	1	240	120
Electrical Resistivity ( $\Omega m$ )	$1 \times 10^{-5}$	$1 \times 10^{-5}$	$5 \times 10^{-9}$	$1 \times 10^{-4}$
seebeck coefficient ( $\mu V/K$ )	-230	180	3.5	-1

### 3. Results and Discussion

Numerical simulation is carried out by using a finite element package ANSYS. The following steps are used to carry out the thermoelectric system analysis: set first

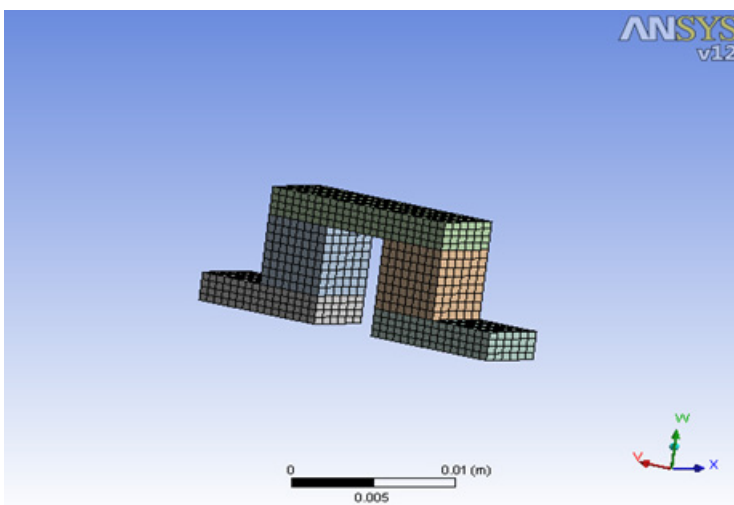


**Figure 2.** (a) Computational mesh for Bi-Te module.

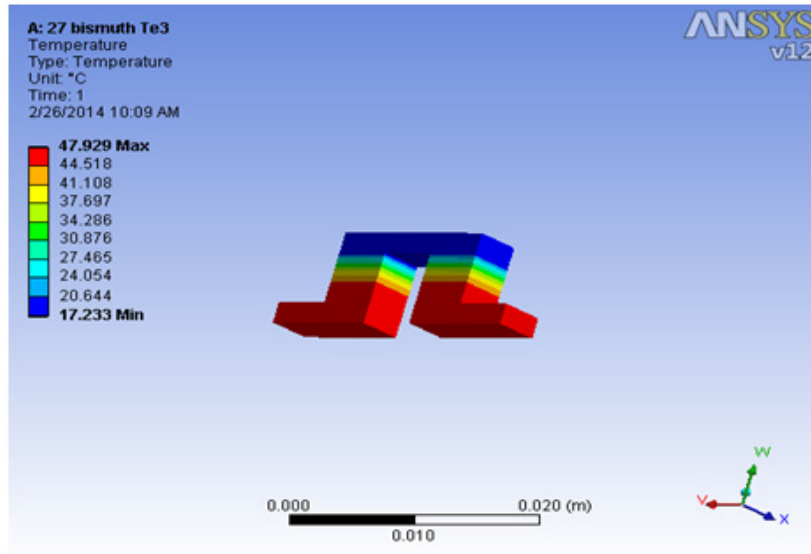


Figure 2. (b) Temperature distribution of Bi-Te module.

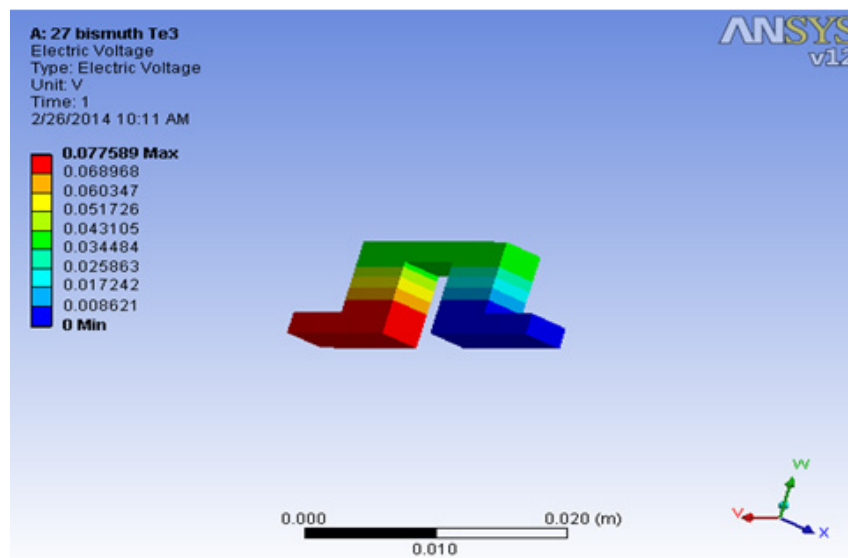


Figure 2. (c) Voltage distribution Bi-Te module.

start the work bench preferences, define the element type and add copper alloy to engineering data, define element coordinate system, set the real constants and material properties, create the geometry, set the current, voltage, hot and cold side temperature. The software includes three elements which are used in modeling the thermoelectricity phenomenon<sup>3-5</sup>.

The different physics regions in the model are meshed, using the finite element method. Obtain the solution, review the results.

After generating the mesh, the electrical load and boundary conditions are specified for the model. The

temperature was varied from 293 K to 328 K, between the cold and hot side of the model. The electrical load of 0.5A to 4 A was applied on the vertical face of the copper base across the thermoelectric system. A very low convection loss of  $1e-6 \text{ W}/(\text{m K})$  was applied on all other surfaces, which ensured the adiabatic heat transfer from the cold end to the hot end for the thermoelectric model<sup>6</sup>. The simulation outputs from the model are temperature, heat flow and voltage distribution.

For the Bi-Te and Sb-Te thermoelectric couples, the computationally generated mesh, temperature and voltage. Distributions are shown in Figures 2, 3 and 4 respectively.

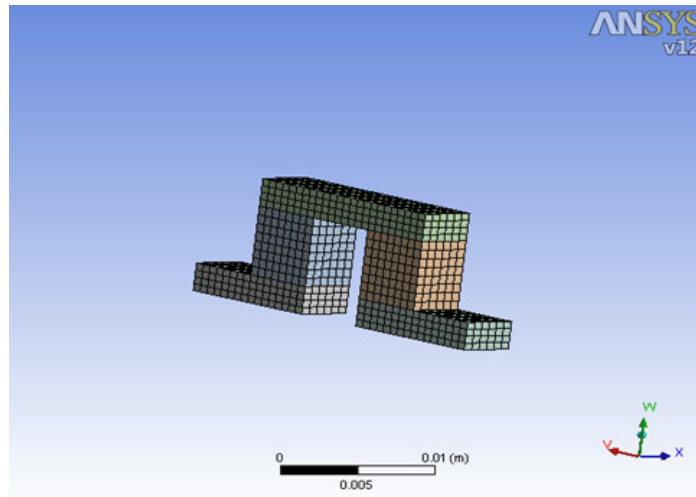


Figure 3. (a) Computational mesh for Sb-Te module.

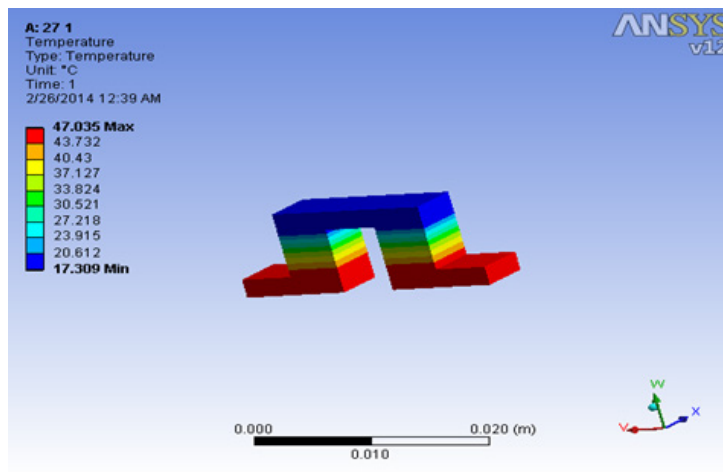


Figure 3. (b) Temperature distribution of Sb-Te module.

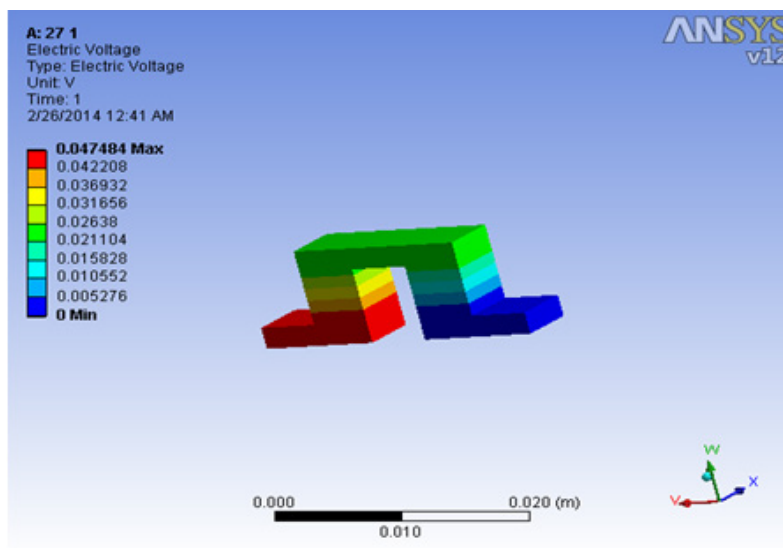


Figure 3. (c) Voltage distribution Sb-Te module.

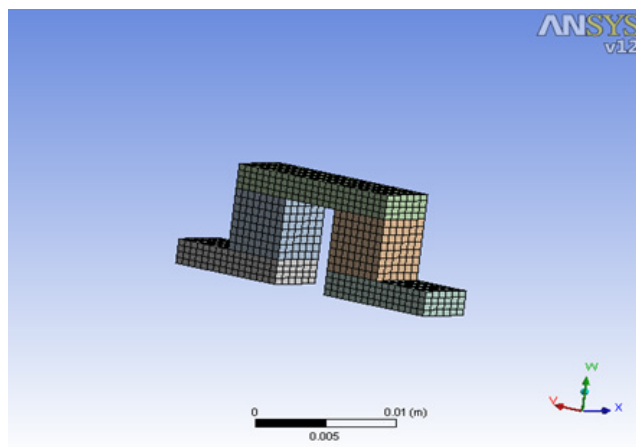


Figure 4. (a) Computational mesh Bi-Te/Sb-Te module.

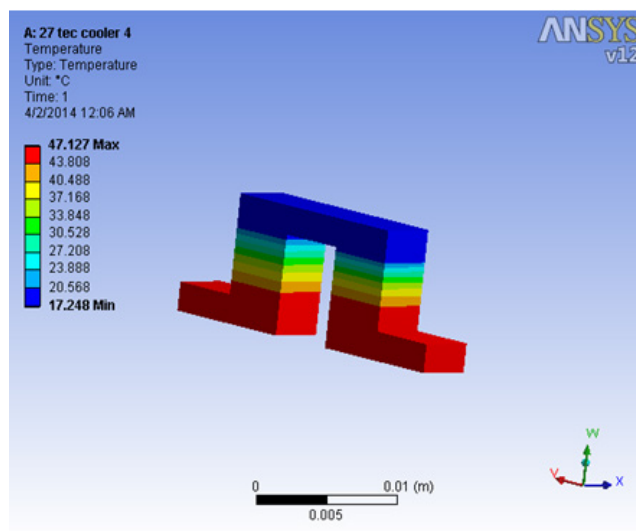


Figure 4. (b) Temperature distribution of Bi-Te/Sb-Te module.

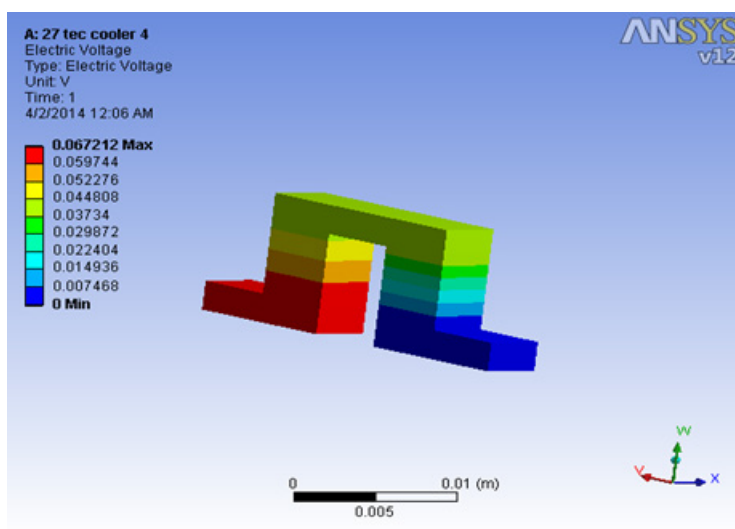


Figure 4. (c) Voltage distribution Bi-Te/ Sb-Te module.

The variation of the COP for the thermoelectric element with current is shown in Figures 5, 6 and 7 respectively<sup>7-9</sup>. It is found that the COP increases till an optimum current is reached and then decreases with further increase in the current. A maximum COP of 4.51 and 1.2 were obtained for the Bi-Te and Sb-Te systems at 10 K differential temperature.

The Bi-Te couple has 43.46% higher COP when compared to the Sb-Te couple under the same operating conditions. The optimal COP decreases with an increase in the differential temperature, as shown in Figure 6. The variation of the optimal current with differential temperature. The optimal current for the maximum COP increases with an increase in the differential temperature.

The variation of the optimal heat absorbed with differential temperature<sup>10,11</sup>. The amount of heat absorbed (QC) on the cold side increases up to the optimal temperature difference and then decreases with an increase in the differential temperature. A maximum of 0.095 W heat is absorbed at the temperature difference of 25 K in the Bi-Te system, which is 28.42 % higher compared to that of the Sb-Te system. The variation of the optimal voltage with differential temperature is shown in Figure 9. The voltage drop for the Bi-Te and Sb-Te modules is 52 mV and 43 mV respectively when operating at 25K temperature difference and it increases with an increase in the differential temperature<sup>12,13</sup>.

## 4. Conclusion

A study on the behavior of the thermoelectric refrigeration system was carried out using ANSYS software. The Governing equations were transformed into algebraic equations via FEM discretization technique. Bi-Te and Sb-Te semiconductor materials were considered for the analysis. The result shows that the COP of the thermoelectric refrigeration system decreases with an increase in the temperature difference. The COP of the Bi-Te system is 13.46 % higher than that of the Sb-Te system, under the same operating conditions. The optimal current and voltage increase linearly with an increase in the differential temperature. The heat absorbed on the cold side reaches the maximum at an optimal temperature difference; a maximum of 0.095 W heat was absorbed at the temperature difference of 25 K in the Bi-Te system, which is 28.42 % higher compared to that of the Sb-Te system. It was concluded that even though the Figure of Merit is higher for Sb-Te in the temperature range

of at room temperature, it shows a lower performance compared to Bi-Te, when it is operated at ambient temperature conditions. Hence, Bi-Te is considered as the better choice for ambient applications, while Sb-Te better for high temperature applications.

## 5. References

1. Astrain DA, Vian JG, Albizua J. Computational model for refrigerators based on peltier effect application. *Applied Thermal Engineering*. 2005 Dec; 25(17-18):3149-62.
2. Chein R, Huang G. Thermoelectric cooler application in electronic cooling. *Applied Thermal Engineering*. 2004 Oct; 24(14-15):2207-17.
3. Subhashree AR, Shanthi B, Parameaswari PJ. The Red Cell Distribution width as a sensitive biomarker for assessing the pulmonary function in automobile welders- a cross sectional study. *Journal of Clinical and Diagnostic Research*. 2013 Jan; 7(1):89-92. ISSN : 0973 - 709X.
4. Goktun S. Design consideration for a thermoelectric refrigerator. *Energy Conservation Management*. 1995 Dec; 36(12):1197-200.
5. Jugsujinda S, Vora-ud A, Seetawan T. Analysis of thermoelectric refrigerator performance. 2nd International Science, Social-Science, Engineering and Energy Management; 2011. p.154-9.
6. Kalaiselvi VS, Saikumar P, Prabhu K, Prashanth Krishna G. The anti Mullerian hormone-a novel marker for assessing the ovarian reserve in women with regular menstrual cycles. *Journal of Clinical and Diagnostic Research*. 2012 Dec; 6(10): 1636-9. ISSN : 0973 - 709X.
7. Lee HS. *Thermal design*. New Jersey: John Wilwy and Sons Ltd; Hoboken. 2010.
8. Jayaraman B, Valiathan GM, Jayakumar K, Palaniyandi A, Thenumgal SJ, Ramanathan A. Lack of mutation in p53 and H-ras genes in phenytoin induced gingival overgrowth suggests its non cancerous nature. *Asian Pacific journal of cancer prevention : APJCP*. 2012; 13(11): 5535-8.
9. Virjoghe EO, Enescu D, Ionel M, Stan MF. Numerical simulation of thermoelectric system. *Latest Trends on Systems*. 2010; 2:630-5.
10. Seetawan T, Seetawan U, Ratcheting A, Srichai S, Singsoog K, Namhongsa W, Ruttanapun C, Siridejachai S. 2012.
11. Gopalakrishnan K, Prem Jeya Kumar M, Sundeep Aanand J, Udayakumar R. Analysis of static and dynamic load on hydrostatic bearing with variable viscosity and pressure. *Indian Journal of Science and Technology*. 2013; 6(S6):4783-8. ISSN : 0974-6846.
12. Thermoelectric generator by finite element Method. *Proceedings of the 1st International Science, Social Science, Engineering and Energy Conference*. p. 1006-11.
13. Srinivasan V. Analysis of static and dynamic load on hydrostatic bearing with variable viscosity and pressure. *Indian Journal of Science and Technology*. 2013 Jun; 6(S6):4777-82. ISSN : 0974-6846.